Macromolecules

Volume 41, Number 7 April 8, 2008

Communications to the Editor

Real-Time Crystallization of Organoclay Nanoparticle Filled Natural Rubber under Stretching

Javier Carretero-Gonzalez,[†] Raquel Verdejo,[†] Shigeyuki Toki,[‡] Benjamin S. Hsiao,[‡] Emmanuel P. Giannelis,[§] and Miguel A. López-Manchado*,[†]

Institute of Polymer Science and Technology, CSIC, Madrid 28006, Spain; Department of Chemistry, Stony Brook University, Stony Brook, New York 11794-3400; and Department of Material Science and Engineering, Cornell University, Ithaca, New York 14853

Received December 21, 2007
Revised Manuscript Received February 20, 2008

Polymer nanocomposites (PNCs) represent a new class of materials compared to conventional filled polymers or polymer blends, as they can possess enhanced properties through nanoscale reinforcement.[1] Widespread interest in PNCs over the past several years has been fueled by their promise of unprecedented performance, design flexibility, and lower cost. A great deal of effort has been devoted to understanding the reinforcing mechanism of PNCs containing highly anisotropic nanofillers such as nanoclays.[2] In this study, we present experimental evidence of a remarkable enhancement of strain-induced crystallization in natural rubber (NR) nanocomposite under uniaxial stretching due to the presence of nanoclay particles. By using synchrotron wide-angle X-ray diffraction (WAXD), we have monitored the structure changes and crystallinity development during deformation in real time. The behavior of significantly enhanced strain-induced crystallinity in organoclay/NR nanocomposites has not been observed before in systems containing conventional fillers. This effect might be responsible for the observed enhancement in mechanical properties of organoclay/NR nanocomposites.[3] The results suggest a dual crystallization mechanism in nanocomposites, which is absent in the unfilled system. The mechanism consists of spatial reorganization of organoclay at low strains (e.g., less than $\alpha = 3$), followed by rapid strain-induced crystallization of NR. The observed in-situ structure changes in NR nanocomposite enable us to suggest a mechanism that may be universal to crystallizable elastomers containing nanosized fillers.

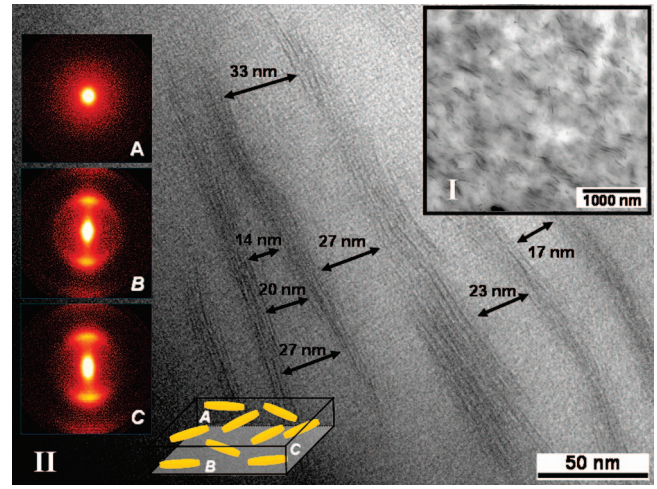

Figure 1. Representative TEM images (I: scale bar 1000 nm; II: scale bar 50 nm) and SAXS patterns (A: face-on view; B and C: edge-on views) of the NR−NC1 nanocomposite.

Layered-silicate nanofillers can improve the physical, mechanical, and thermal properties of polymeric matrices.[4] This behavior has been explained by the formation of a reinforcing nanofiller network (exfoliated or/and intercalated), within which the polymer chains are confined. However, this explanation is not sufficient to paint a complete picture of the reinforcing mechanism taking place in many systems. For example, Giannelis and co-workers[5,6] have reported a unique class of semicrystalline and amorphous nanocomposites having toughness values 1 order of magnitude higher than that of the unfilled polymer matrix. They suggested that the presence of nanoparticles introduces new energy-dissipating mechanisms, and they attributed the mechanical property enhancement to the nanoparticle mobility and orientation during deformation. A study by Joly et al.[7] using birefringence and infrared dichroism on

* To whom correspondence should be addressed: Tel +34 912587424, Fax +34 915 644 853, e-mail lmanchado@ictp.csic.es.
[†] CSIC.
[‡] Stony Brook University.
[§] Cornell University.

10.1021/ma7028506 CCC: $40.75
Published on Web 02/29/2008

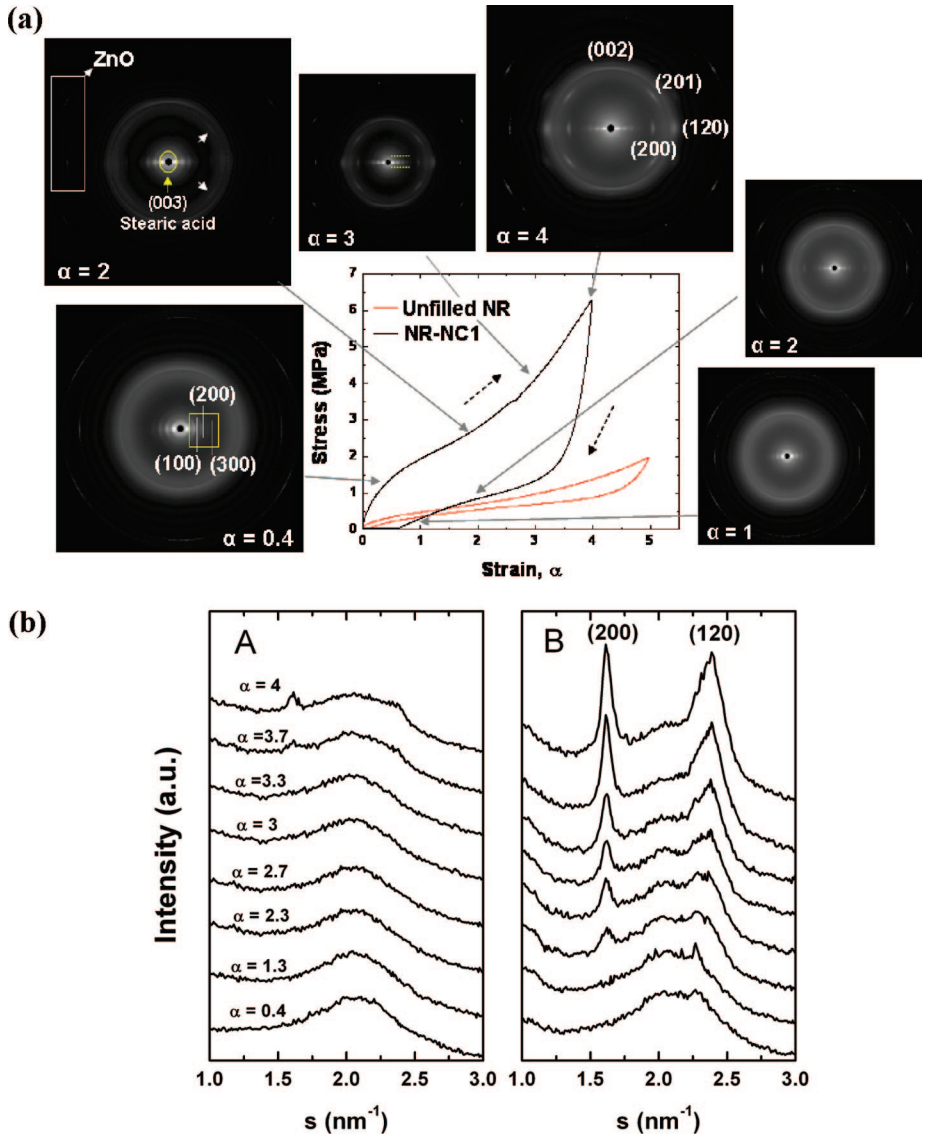

Figure 2. WAXD results for NR−NC1 nanocomposites. (a) Stress–strain curve and selected synchrotron WAXD patterns during extension and retraction cycles. (b) Integrated and corrected intensity profiles from the 2D WAXD patterns at various strains as a function of scattering vector *s* (nm^{-1}).

organoclay/NR nanocomposites also reported a higher orientation of amorphous chains by the addition of nanoclays. However, they did not consider the behavior of strain-induced crystallization in NR, which is the dominant effect in mechanical reinforcement.

The purpose of this study was to investigate the effects of organoclay on strain-induced crystallization under uniaxial stretching in crystallizable natural rubber nanocomposites. In-situ experiments were carried out to couple the stress–strain behavior with structure determination using synchrotron wide-angle X-ray diffraction (WAXD). This method enabled us to monitor the changes at the local molecular structure during deformation in real time.[8]

Two NR/organoclay nanocomposites, NR−NC1 (NC1-filled NR (15 phr)) and NR−NC2 (NC2-filled NR (15 phr)) were prepared by mechanical mixing at room temperature and vulcanized at 150 °C. NC1 is a quaternary ammonium salt modified montmorillonite with a basal distance of 29.4 Å. NC2 was prepared from NC1 after Soxhlet extraction to remove excess surfactant (~6.2 wt %) from the clay. Both nanocomposite samples exhibit an intercalated structure as observed by WAXD (data not shown). Transmission electron microscopy (TEM) (Figure 1) confirmed the presence of finely dispersed tactoids (nanoclay stacks) spaced 10−40 nm apart. In addition, directional small-angle X-ray scattering (SAXS) measurements (A: face-on view; B and C: edge-on views) of the unstretched but pressed specimen showed the preferred orientation of nanoclay stacks aligned parallel to the film plane due to processing. Figure 2a shows the stress–strain curve and corresponding 2D WAXD patterns at selected strains during stretching and retraction for the NR−NC1 nanocomposite. The corresponding stress–strain curve for the unfilled NR is included for comparison. Figure 2b illustrates the normalized and corrected linear diffraction profiles for unfilled NR (A) and the NR−NC1 nanocomposite (B). All images at high strains exhibited preferred orientations of (100), (200), and (300) reflections from layered silicates, indicating that nanoclays became highly orientated along the stretching direction. The orientation began at a relatively low strain ($\alpha = 0.4$) and increased progressively until a maximum alignment was reached (at $\alpha = 4$). In addition to the orientation of nanoclays, WAXD images clearly revealed the strain-induced crystallization of natural rubber chains, which was evidenced by the alignment of (200) and (120) reflections from the rubber matrix. It is

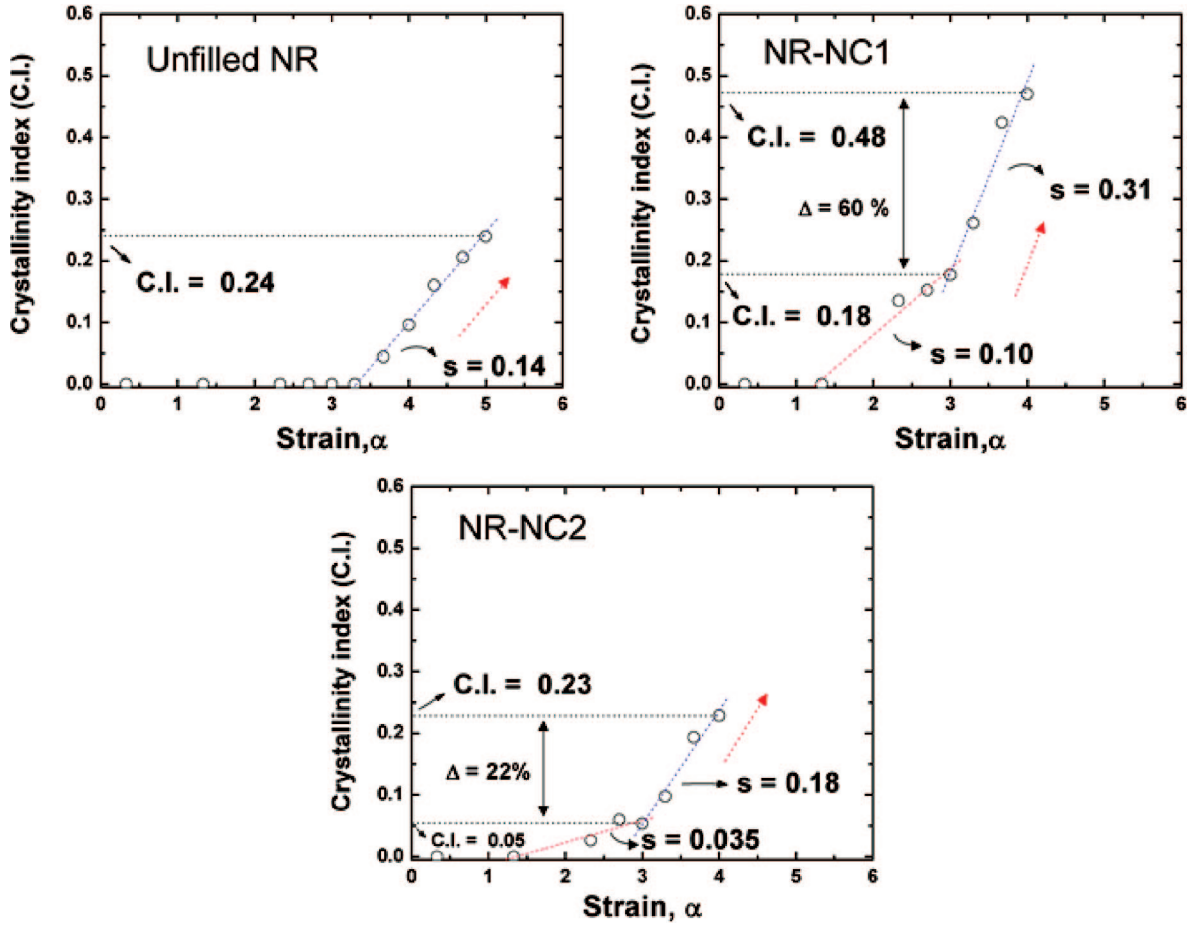

Figure 3. Crystallinity index as a function of strain during the first stretch cycle.

interesting to note that the crystal reflections of NR appeared at a lower strain in the nanocomposite compared to the unfilled NR. In addition, we did not observe strong evidence for orientation of the amorphous phase based on the WAXD analysis. If there was some oriented amorphous phase, the total fraction was small. This is in slight contrast with the study by Rault et al.,[9] who have demonstrated orientation of the amorphous phase using ^{2}H NMR.

Figure 3 shows the evolution of crystallinity index (CI) as a function of strain for the unfilled NR and the nanocomposites. The results indicate that the onset strain (α^0) of deformation-induced crystallization was 3.3 and 1.2 for the unfilled sample and nanocomposites, respectively. The overall crystallinity index was significantly higher in the nanocomposite than in the unfilled sample (e.g., the maximum strain-induced crystallinity in unfilled NR was 25% at a strain $\alpha = 5$[8] while the maximum strain-induced crystallinity in the NR−NC1 nanocomposite was 48% at a strain $\alpha = 4$). In systems containing conventional fillers such as carbon black, silica, or calcium carbonate a lowering of the threshold ($\alpha^0 = 2$) has been reported, but no differences in the overall crystallinity index were observed.[10−12] The difference between these traditional fillers and nanoclays is due to the very high surface-to-volume ratio of 10^3-10^4 m^2/mL for nanoclays compared to $10^{-1}-10^2$ m^2/mL for conventional fillers.[2b] Hence, the observed different behavior can be attributed to the high interfacial interactions between the polymer matrix and the nanoclays, resulting in a more efficient transfer of stress across the matrix. The large interfacial region can lead to an early orientation of polymer chains, thus promoting nucleation under stretching.

Our experiment also revealed a different strain-induced crystallization mechanism of NR in the presence of nanoclays. Unfilled NR usually shows a single crystallization step,[8] while the NR nanocomposites exhibit two well-defined crystallization steps: the first one for $\alpha < 3$ is related to the orientation and alignment of nanoclays during elongation forming a physical network while the second ($3 \leq \alpha \leq 4$) corresponds to the conventional crystallization mechanism of unfilled NR,[13] but with a crystallinity index and strain slope approximately twice that of the pristine sample.

Another interesting aspect of our results is the effect of the amount of surfactant on the clay on the behavior of strain-induced crystallization in NR nanocomposites. The quantitative analysis of the WAXD data for NR−NC1 and NR−NC2 samples (Figure 3) revealed that the onset strain ratio did not change in the two nanocomposites. However, the crystallinity index strongly depended on the amount of surfactant. The maximum crystallinity for NR−NC1 and NR−NC2 is 50 and 25%, respectively. This different crystallinity in the nanocomposites can be related to the crystallizability of the NR chains (both nanocomposites showed two crystallization steps, but their slopes were quite different). In the first crystallization step, the NR−NC1 nanocomposite exhibited a slope about 1 order of magnitude higher than the NR−NC2, while the slope of the second step in NR−NC1 was also twice that of NR−NC2. The change in the crystallizability may be attributed to the higher amount of surfactant molecules surrounding the NC1 fillers, resulting in a greater enhancement of chain mobility for crystallization.[14]

In summary, we conclude from this study that the presence of interfacial interactions between nanoparticles (i.e., nanoclays)−polymer matrix and the enhanced mobility of the polymer on the clay surface are crucial in promoting strain-induced crystallization in natural rubber nanocomposites. Addition of nanoclay leads to significantly enhanced crystallinity and lower onset strain for stretch-induced crystallization compared to conventionally filled NR composites.

Acknowledgment. The authors gratefully acknowledge the financial support of the Spanish Ministry of Education (MEC) through its project MAT 2004-00825. J. Carretero-González thanks the Spanish Ministry of Education (MEC) for the concession of a FPI grant, and R. Verdejo also acknowledges a Juan de la Cierva contract from the MEC. B. S. Hsiao also acknowledges the support by the NSF (DMR-0405432).

Supporting Information Available: Nanocomposites preparation and characterization details and synchrotron measurement conditions and analysis. This material is available free of charge via the Internet at http://pubs.acs.org.

References and Notes

(1) Winey, K. I.; Vaia, R. A. *MRS Bull.* **2007**, *32*, 214.
(2) (a) Fornes, T. D.; Paul, D. R. *Polymer* **2003**, *44*, 4993. (b) Vaia, R. A. *Mater. Today* **2004**, *7*, 32. (c) Sheng, N.; Boyce, M. C.; Parks, D. M.; Rutledge, G. C.; Abes, J. I.; Cohen, R. E. *Polymer* **2004**, *45*, 487. (d) Rao, Y. Q.; Pochan, J. M. *Macromolecules* **2007**, *40*, 290.
(3) Arroyo, M.; Lopez-Manchado, M. A.; Herrero, B. *Polymer* **2003**, *44*, 2447.
(4) For comprehensive reviews on polymer−clay nanocomposites the reader is referred to: (a) Giannelis, E. P. *Adv. Mater.* **1996**, *8*, 29. (b) Giannelis, E. P.; Krishnamoorti, R.; Manias, E. *Adv. Polym. Sci.* **1999**, *138*, 107. (c) Pinnavaia, T. J.; Beall, G. W. *Polymer-Clay Nanocomposites*; John Wiley & Sons: New York, 2000. (d) Alexandre, M.; Dubois, P. *Mater. Sci. Eng.* **2000**, *28*, 1. (e) Ray, S. S.; Okamoto, M. *Prog. Polym. Sci.* **2003**, *28*, 1539. (f) Okada, A.; Usuki, A. *Macromol. Mater. Eng.* **2006**, *291*, 1449.
(5) Shah, D.; Maiti, P.; Gunn, E.; Schmidt, D. F.; Jiang, D. D.; Batt, C. A.; Giannelis, E. P. *Adv. Mater.* **2004**, *16*, 1173.
(6) Shah, D.; Maiti, P.; Jiang, D. D.; Batt, C. A.; Giannelis, E. P. *Adv. Mater.* **2005**, *17*, 525.
(7) Joly, S.; Garnaud, G.; Ollitrault, R.; Bokobza, L.; Mark, J. E. *Chem. Mater.* **2002**, *14*, 4202.
(8) Toki, S.; Sics, I.; Ran, S.; Liv, L.; Hsiao, B. S.; Murakami, S.; Senoo, K.; Kohjiya, S. *Macromolecules* **2002**, *35*, 6578.
(9) Rault, J.; Marchal, J.; Judeinstein, P.; Albouy, P. A. *Eur. Phys. J. E* **2006**, *21*, 243.
(10) Poompradub, S.; Tosaka, M.; Kohjiya, S.; Ikeda, Y.; Toki, S.; Sics, I.; Hsiao, B. S. *J. Appl. Phys.* **2005**, *97*, 103529.
(11) Trabelsi, S.; Albouy, P. A.; Rault, J. *Macromolecules* **2003**, *36*, 9093.
(12) Chenal, J. M.; Gauthier, C.; Chazeau, L.; Guy, L.; Bomal, Y. *Polymer* **2007**, *48*, 6893.
(13) Tosaka, M.; Murakami, S.; Poompradub, S.; Kohjiya, S.; Iheda, Y.; Toki, S.; Sics, I.; Hsiao, B. S. *Macromolecules* **2004**, *37*, 3299.
(14) Manias, E.; Chen, H.; Krishnamoorti, R.; Genzer, J.; Kramer, E. J.; Giannelis, E. P. *Macromolecules* **2000**, *33*, 7955.

MA7028506